

Accepted Manuscript

Effect of surface and subsurface heterogeneity on the hydrological response of a grassed buffer zone

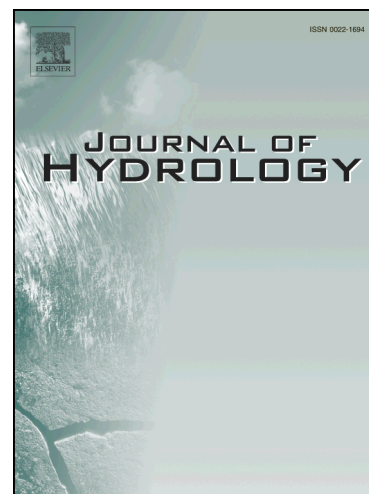
Laura Gatel, Claire Lauvernet, Nadia Carluer, Claudio Paniconi

PII: S0022-1694(16)30592-3

DOI: <http://dx.doi.org/10.1016/j.jhydrol.2016.09.038>

Reference: HYDROL 21534

To appear in: *Journal of Hydrology*



Please cite this article as: Gatel, L., Lauvernet, C., Carluer, N., Paniconi, C., Effect of surface and subsurface heterogeneity on the hydrological response of a grassed buffer zone, *Journal of Hydrology* (2016), doi: <http://dx.doi.org/10.1016/j.jhydrol.2016.09.038>

This is a PDF file of an unedited manuscript that has been accepted for publication. As a service to our customers we are providing this early version of the manuscript. The manuscript will undergo copyediting, typesetting, and review of the resulting proof before it is published in its final form. Please note that during the production process errors may be discovered which could affect the content, and all legal disclaimers that apply to the journal pertain.

Effect of surface and subsurface heterogeneity on the hydrological response of a grassed buffer zone

Laura Gatel^{a,b,*}, Claire Lauvernet^a, Nadia Carluer^a, Claudio Paniconi^b

^a*Irstea, 5 rue de la Doua, 69100 Villeurbanne, France*

^b*INRS-ETE, Université du Québec, 490 rue de la Couronne, Quebec City G1K 9A9, Canada*

Abstract

Grassed buffer zones are an effective method to reduce contaminant impacts on aquatic environments. The general objective of this study is to explore the impact of both surface and subsurface heterogeneity on the hydrological responses of a vegetative buffer strip. Heterogeneity is described by two variables, microtopography and saturated hydraulic conductivity. Numerous surface and subsurface heterogeneity scenarios were simulated with a physically-based numerical model of coupled surface/subsurface processes. The scenarios were evaluated relative to data from an experimental vegetative filter in a Beaujolais vineyard, France. The subsurface scenarios show that conductivity heterogeneity plays a key role on the buffer strip's capacity to infiltrate incoming surface runoff and on the ensuing runoff pathways. The conjunctive surface and subsurface scenarios indicate that microtopography variability is comparatively less influential on the hydrological interactions and pathways within the buffer strip, and that representing this heterogeneity via appropriate statistical distributions can be a good assumption in practice.

Keywords: Surface–subsurface coupled modeling, spatial heterogeneity, vegetative buffer strip, saturated hydraulic conductivity, microtopography

1. Introduction

Non-point source pollution due to contaminant transfer from agricultural fields to aquatic environments is still a major environmental problem. Amongst best management practices, landscape elements such as fences or buffer strips can help mitigate this transfer. In particular, vegetative buffer strips between crops and rivers are becoming mandatory in several countries [1, 2]. Such grassed zones create a fostering area for infiltration, sedimentation, adsorption and degradation [3, 4]. Within these zones, water, pesticide and sediment behaviours are complex, especially concerning runoff, surface lateral transfers and surface–subsurface interactions [5, 6]. The sizing and placement of grassed buffer zones in a watershed requires a correct understanding and quantification of these complex processes. A first approach for doing this is via field experiments. For

*Corresponding author

Email address: laura.gatel@irstea.fr (Laura Gatel)

example, [7] showed on their experimental vegetative filter (Beaujolais vineyard, France) that buffer efficiency for a moderately soluble contaminant (Diuron) is related to two main mechanisms: water runoff infiltration and contaminant retention in the superficial soil horizons. These results are related to a specific context: the hillslope is steep (25% slope), with a highly permeable sandy clay topsoil overlying a granitic sand formation that induces lateral subsurface fluxes. This field study showed that permeability has a dominant influence on hydrological behaviour and buffer strip efficiency, but the results are not easily transferable to other sites characterized by different soil types, climate conditions and agricultural practices [8, 1].

Physically-based models represent a second approach for the detailed investigation of the processes and dynamics associated with buffer strips. They allow us to describe the relevant physics with more detail and accuracy than conceptual models, which is necessary to study complex and interacting processes. For example the models GRASS [9], VFSMOD [10] and HYDRUS [11, 12, 13] have all been used to simulate water behaviour in vegetative strips [14, 6] and to assist in the design of these buffer zones [3]. In modelling studies, saturated hydraulic conductivity (K_s) is generally found to be the most influential parameter on infiltration [10, 15, 16]. This confirms the finding from other study sites and scales that K_s is dominant for relatively wet soils [17, 18, 19, 20], whereas saturated soil water content is the most influential parameter under dry soil conditions [21, 22, 23].

Another parameter that can be highly influential in the context of vegetative buffer strips but that has been much less studied than K_s is microtopography, which is defined here as the soil surface variation from the 1 cm to 1 m scale [24, 25, 26]. Measuring these two parameters that are representative of subsurface (K_s) and surface (microtopography) heterogeneity is costly, time-consuming and uncertain [27], since both are known to be highly variable horizontally and vertically [28, 29, 30]. Subsurface heterogeneity is highly influential on water movement, and thus solute transfer. On the surface, both K_s and microtopography play a key role in regulating surface runoff spatial distribution and intensity [31, 32]. In their review of uncertainty in soil physical properties, [33] summarize the assessment of horizontal saturated hydraulic conductivity autocorrelation from the literature: it can vary from 1 m [34, 30] to 120 m [35] for field areas from 0.25 ha [36] to 14 ha [35]. The land surface heterogeneity effect has been much less studied, but according to [37] and [38], ignoring small scale dynamics by representing complex slopes as smooth landforms leads to an inaccurate representation of the hydrological response.

Even when heterogeneity is recognized, one challenge is to define it properly for modelling. The study scale is an important factor to consider before trying to take into account the heterogeneity. For example, [39] shows that a spatial variability that is significant at the 12 m² scale can be described as random in larger scale models. Other studies have dealt with heterogeneity by upscaling soil property variability from fine scale to larger areas [e.g., 40].

When K_s heterogeneity is represented in studies, it is via a lognormal distribution per layer [41] or even

for the whole soil [42, 43, 44, 45], with the challenge being to define the relevant correlation scale, which is also dependent on the study scale [33]. For microtopography, most hillslope scale studies describe it with a Gaussian distribution [46, 47, 48, 49], despite recognition that the degree and structure of this heterogeneity are scale and time dependent [50, 51]. The influence of both K_s and microtopographic heterogeneity in modelling has never been studied simultaneously despite being recognized as an important factor for improving models [52]. Today, with more attention given to integrated water resources management and with the emergence of detailed process-based models for simulating surface-subsurface interactions [53], the roles of surface and subsurface heterogeneity need to be jointly examined.

The general objective of this study is to assess the impact of both surface and subsurface heterogeneity, characterized by microtopography and saturated hydraulic conductivity, on the hydrological responses and interactions that occur in a vegetative buffer strip. The insights gained should help improve model parameterization schemes. We use the physically-based coupled hydrological model CATHY [54] applied to the experimental buffer strip from [6]. The hydrological responses considered include surface runoff pathways and outputs, infiltration to the subsurface, and water volume partitioning between surface and subsurface (both saturated and unsaturated) domains. The intent was not to precisely model this specific vegetative buffer strip, but rather to rely on the experimental data to ensure that the simulated results are realistic. In a first step, we assess the effect of K_s heterogeneity on surface and subsurface hydrological fluxes by applying the CATHY model with several K_s distribution scenarios to an artificial runoff event and a natural rain and runoff event. In the second step of the study, the effects of microtopography coupled to K_s heterogeneity on the hydrological responses of the buffer strip are examined.

2. Material and methods

2.1. CATHY model

The CATHY (CATchment HYdrology) model [55, 54] is a physically-based model that simulates surface and subsurface water flows and their interactions in three dimensions. It integrates the 3D Richards equation for variably saturated porous media and a 1D diffusive wave equation, which is a simplification of Navier-Stokes equations, to describe surface flow through overland and stream channel networks:

$$S_w S_s \frac{\partial \psi}{\partial t} + \phi \frac{\partial S_w}{\partial t} = \nabla [K_s K_r (\nabla \psi + \eta_z)] + q_{ss} \quad (1)$$

$$\frac{\partial Q}{\partial t} + c_k \frac{\partial Q}{\partial s} = D_h \frac{\partial^2 Q}{\partial s^2} + c_k q_s(h, \psi) \quad (2)$$

where S_w [–] is the water saturation ($S_w = \frac{\theta}{\phi}$), θ [–] is the volumetric moisture content, ϕ [–] is the saturated moisture content or the porosity, S_s [L⁻¹] is the aquifer specific storage, ψ [L] is the pressure head, t [T] is

time, ∇ [L^{-1}] is the gradient operator, K_s [$L.T^{-1}$] is the saturated hydraulic conductivity, K_r [–] is the relative conductivity, $\eta_z = (0, 0, 1)$, z [L] is the vertical coordinate directed upward, q_{ss} [$L^3.L^{-3}.T$] is a source (positive) or sink (negative) term that includes the exchange fluxes from the surface to the subsurface, Q [$L^3.T^{-1}$] is the discharge (volumetric flow) along the overland and channel network, s [L] is the coordinate direction for each segment of the overland and channel network, c_k [$L.T^{-1}$] is the speed of the kinematic wave, D_h [$L^2.T^{-1}$] is the hydraulic diffusivity, h [L] is the height of the surface water (ponding head at the surface, representing state variable continuity with subsurface head) and q_s [$L^3.L^{-1}.T$] is the inflow or outflow rate from the subsurface to the surface.

Equations (1) and (2) are solved on a regular mesh at the surface that is replicated vertically to form a 3D tetrahedral mesh. The vertical layers can be of varying thickness, and different soil hydraulic properties can be assigned to each node of the mesh. Boundary conditions and atmospheric forcing can be dynamically prescribed. The surface mesh for the routing equation (2) is generated in a preprocessing step that establishes the flow paths (s directions) from topographic analysis of a digital terrain model and partitions the catchment into overland (hillslope) and channel (stream) cells [56]. The coupling between surface and subsurface processes in CATHY involves boundary condition switching according to the balance between atmospheric forcing (rainfall and potential evaporation) and the infiltration or exfiltration soil capacity. More details on the CATHY model can be found in [54].

2.2. Experimental buffer strip

The CATHY model is applied in the frame of several numerical experiments on a steeply sloping (25%) buffer strip monitored by the French research institute on agriculture and environment (Irstea) in the Morcille catchment (surface area of 8 km², in Beaujolais, France) [6, 7]. The soil is a very permeable sandy clay with a deep and filtering texture of 2 m depth overlying a granitic sand formation. The hydrodynamic properties of the three soil horizons that make up the soil profile were measured by [6] and are summarized in Table 1. K_s measurements were only made to a depth of 0.4 m, and the values at this depth were used for horizon 3. The climate is continental with Mediterranean influence according to the Koppen-Geiger classification [57], with an annual average rainfall of 860 mm (years 1992-2010) [58]. The instrumented section of the buffer strip has a surface area of 25.2 m² (4 m wide by 6.3 m long) while the entire strip is 24 m long and is located between a vineyard plot and the Morcille river (Figure 1). Since 1990 a large number of rain and surface runoff natural events as well as some artificial runoff events [7] have been monitored at this experimental site. Rain is measured by a pluviometer and input runoff is fed to the buffer strip via a gutter device (gutter 1 in Figure 1). Several response variables are monitored: infiltration volumes with lysimeters at 50 cm depth (there are four of them, each composed of two receptacles, at 0.5 m, 2 m, 4 m and 6 m downslope from gutter 1), output runoff collected in a second gutter (gutter 2 in Figure 1) and surface runoff propagation with a granular matrix sensor (GMS), which is useful for measuring the soil matrix potential [59].

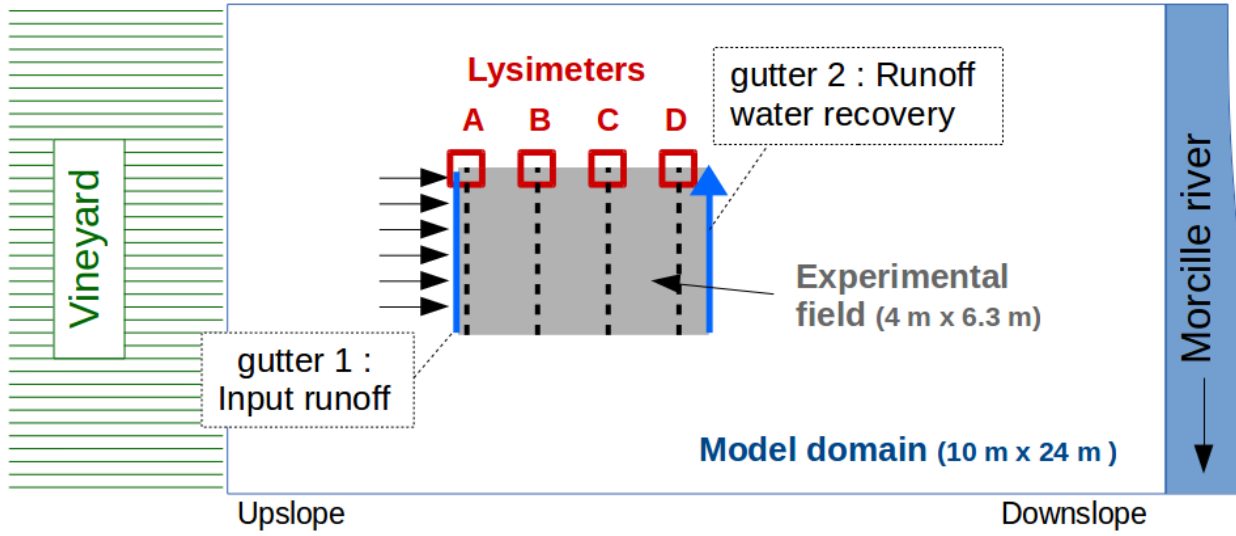


Figure 1: Schematic representation of the experimental plot (in grey) on the vegetative buffer strip in grey (Morcille, Beaujolais) with the runoff input and runoff collection gutters and the four lysimeters (A, B, C and D, respectively located at 0.5 m, 2 m, 4 m and 6 m downslope from gutter 1).

Table 1: Soil hydrodynamic properties for the Morcille buffer strip (after [6]). n , θ_r and ψ_{sat} are the parameters for the van Genuchten [60] soil retention curves. Standard deviation (SD) values are reported when available.

	Horizon 1 (0-10 cm)	Horizon 2 (10-90 cm)	Horizon 3 (90-200 cm)
Porosity ϕ (-)	0.55 (SD: 9 %)	0.42 (SD: 12 %)	0.39
Specific storage coefficient S_s (m^{-1})	$1,0 \times 10^{-5}$		
Saturated conductivity K_s ($m.s^{-1}$)	1.88×10^{-4} (SD: 8 %)	4.0×10^{-5} (SD: 42 %)	1.76×10^{-5} (SD: 88 %)
n (-)	1.46	1.52	1.57
Θ_r (-)	0.15		
ψ_{sat} (m^{-1})	0.0313	0.100	0.143

Two monitored events, one artificial and one natural, that show contrasting hydrological behaviours in terms of duration, intensity and generated runoff (Figure 2) were selected for this study. For the artificial event (2006/04/13), 4.5 m³ of water was introduced as surface runoff through gutter 1 for a period of 40 minutes. For this event the output hydrograph from gutter 2 was monitored but no surface water reached this point. However, GMS data are available to qualitatively describe surface runoff evolution during the event. To evaluate the subsurface flow, infiltration volume in the lysimeters, continuously monitored for 1 h (i.e., until 20 min after the runoff application period), was used.

The natural event (2004/09/12) lasted less than one hour and generated a very short runoff output hydro-

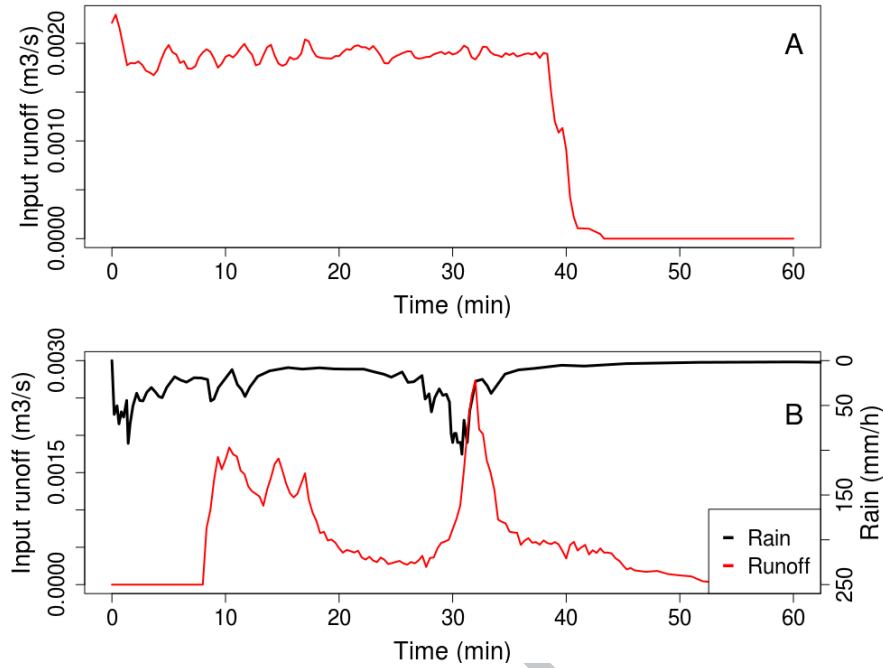


Figure 2: Runoff and rain intensity for the two selected events on the Morcille buffer strip. A: Artificial runoff event (2006/04/13) and B: natural event (2004/09/12).

graph highly connected to the rainfall dynamics (Figure 2 B). The water input for this event included both the precipitation that fell directly on the instrumented field and the runoff input resulting from surface runoff generated on the vineyard plot and collected in gutter 1. In total, 5 m³ of water was introduced, and 0.1 m³ of runoff was collected at gutter 2.

2.3. Simulation plan

The first step of the study aims at understanding the effect of hydraulic conductivity heterogeneity on surface and subsurface fluxes in a buffer strip. We used a homogeneous K_s scenario, a layered (by soil horizon) homogeneous scenario and 5 statistically generated heterogeneous scenarios described in the next section. 60 realizations were performed on each statistically heterogeneous distribution to ensure the stability of the ensemble mean and variance of the response. All simulations were performed for the artificial event of 2006/04/13. The results were evaluated for three output variables: surface water volume at three times; 50 cm depth infiltration at the lysimeter locations; and spatial distributions of surface ponding.

On the basis of the first step analysis, one of the 7 K_s scenarios was selected for the second part of the study, whose aim is to assess also the influence of microtopography. Two microtopography scenarios were generated (see below) and run for 5 realizations from the selected K_s scenario. All simulations, including a third scenario representing the configuration with no microtopography, were performed for the natural event

of 2004/09/12. The same output variables as in step 1 were considered, as well as the surface runoff at gutter 2 (see figure 1).

2.3.1. Scenarios for studying the effect of subsurface heterogeneity

For the homogeneous (H) and layered homogeneous (L) scenarios we used, respectively, the harmonic average of all measured K_s values ($4.64 \times 10^{-5} \text{ m.s}^{-1}$) and of the measured K_s values by soil horizon (see Table 1). The statistically heterogeneous scenarios were generated using the turning bands toolkit of [61] based on the customary lognormal distribution [41, 43, 44], with mean and standard deviation values for each soil horizon corresponding to the measured data reported in Table 1. Five scenarios were defined for the statistically heterogeneous case: 0, 2 and 8 m horizontal correlation length with no enforcement (0NE, 2NE and 8NE) and 2 and 8 m correlation length with enforcement (2E and 8E). For the 2E and 8E scenarios, the K_s distributions were enforced with the measured values (8 points in horizon 1 and 8 points in horizon 2). The sampling is performed with the turning bands method and enforced by kriging. Exact measurement locations are forced to be respected exactly and their neighbour elements are influenced by their value, depending on their distance to the measurements. Table 2 summarizes the 7 K_s scenarios and Figure 3 shows a realization of the K_s distribution for scenario 8E.

Table 2: Summary of the 7 hydraulic conductivity scenarios used in the first step of the study.

Scenario	Distribution	Horizontal correlation length	Enforcement
H	homogeneous	-	-
L	layered homogeneous	-	-
0NE	statistically generated	0 m	no enforcement
2NE		2 m	
8NE		8 m	
2E	heterogeneity	2 m	enforcement
8E		8 m	

2.3.2. Scenarios for studying the effect of both surface and subsurface heterogeneities

Land surface microtopography is highly dependent on soil composition, land use and agricultural practices. In absence of accurate radar or lidar field data, microtopography is generally described using fractal distributions for study scales below 1 m^2 [62, 63, 64] or Gaussian distributions for larger study scales up to 1 ha [65, 46, 51, 47, 48, 49]. In this study we used, based on field observations, a Gaussian distribution with a standard deviation on elevation fluctuations of 3 cm or 6 cm and a mean of zero. A third scenario with no microtopography (corresponding to the hillslope landscape from the first step) was also included in the

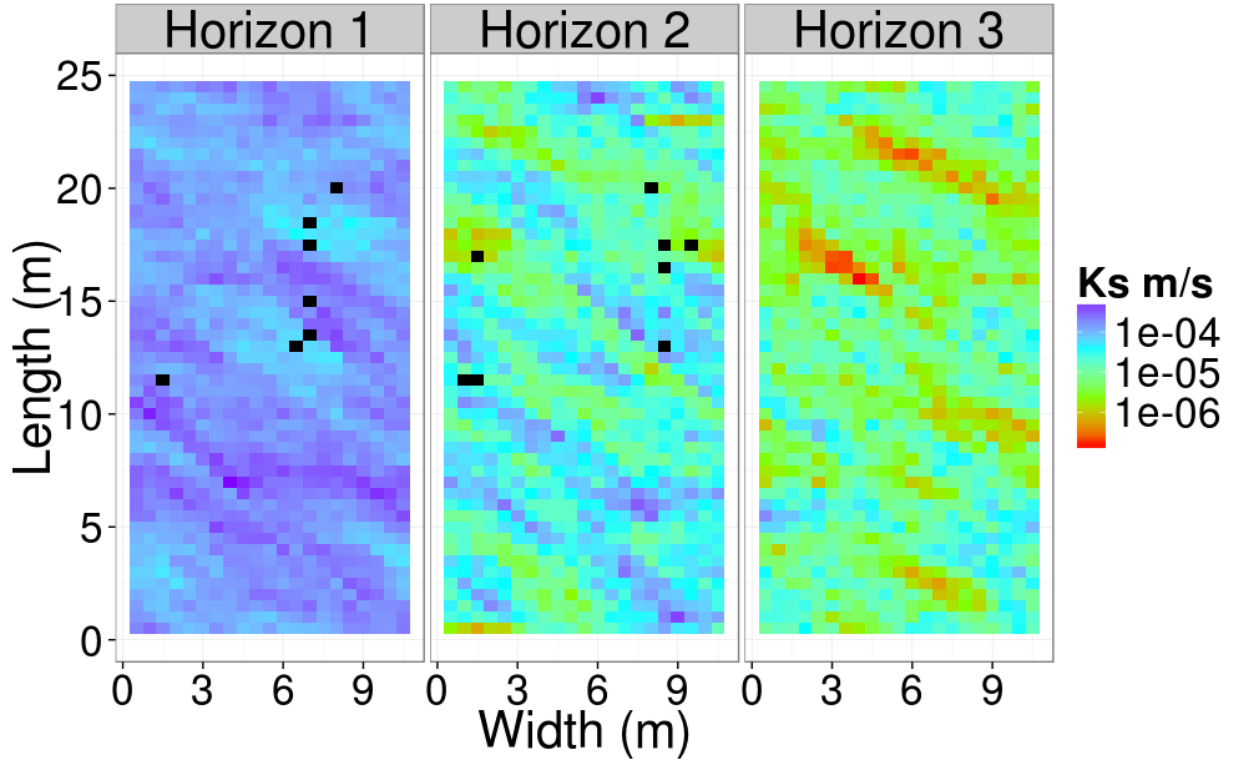


Figure 3: Example realization of a saturated conductivity field with enforcement points in soil horizons 1 and 2 shown in black. The average K_s for horizons 1, 2 and 3 is, respectively, $1.88\text{e-}4$ m/s, $4.00\text{e-}5$ m/s and $1.76\text{e-}5$ m/s.

analysis. For each of these 3 scenarios, 5 realizations of the selected K_s scenario from step 1 were sampled (labeled K_{s1} , ..., K_{s5}). Moreover, for each of the two microtopography distribution scenarios, 5 realizations were sampled (labeled $MT1$, ..., $MT5$).

For all this simulations, the roughness coefficient is kept at the same value because it refers to disturbances or irregularities in the soil surface at a scale which is generally too small to be captured by a conventional topographic map or survey [66]. Manning's coefficient is an important parameter for sediment transfers as well as for solute transport, but only in a context of gentle slope (less than 5%) [67], which is not the case here. Figure 4 shows an example for the 3 cm scenario. The total number of simulations for the surface and subsurface heterogeneity analysis is thus 55 (5 K_s realizations for the no microtopographic relief case plus 5 $K_s \times 5$ MT realizations for each of the 3 cm and 6 cm microtopography cases). No horizontal correlation was used for the microtopography scenarios since observations of the experimental area show that the relief due to grass vegetation is not autocorrelated beyond a length scale of 50 cm, which is the surface mesh size.

2.4. Model setup

In the present study, boundary conditions were assigned according to available field information and were maintained fixed for all simulations. At the upslope lateral boundary, the water table level was maintained at

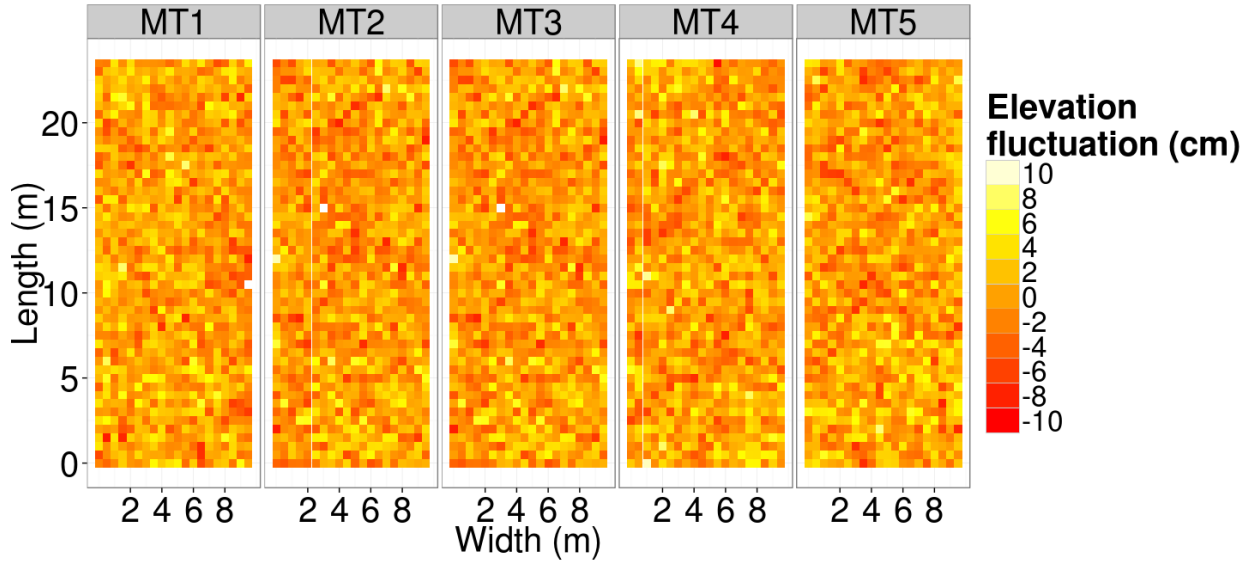


Figure 4: Five realizations of the microtopography field for the scenario with a standard deviation of 3 cm on the elevation fluctuations.

a certain distance below the surface with a Dirichlet condition (fixed hydraulic head), while at the downslope lateral boundary a seepage face was set from 30 cm below the surface to the base of the domain (Figure 5). The initial condition is a hydrostatic equilibrium with a water table matching the upslope boundary condition. The water input was simulated as rainfall on gutter 1 for both the artificial and natural events plus, for the natural event, direct rainfall on the experimental plot as well. The other two lateral boundaries were assigned no flow conditions. Since the simulated domain is larger than the experimental area (see Figure 1), these zero-flux conditions did not unduly influence the simulation results. The land surface was discretized into 20 x 48 uniform cells of 50 cm x 50 cm resolution. For the subsurface model each cell was subdivided into two triangles, and the triangular grid was projected vertically over the 2 m soil depth into 15 parallel layers, to produce a 3D mesh of 28800 tetrahedral elements and 16464 nodes. The 15 layers are of variable thickness from 1 cm to 15 cm, with the thinnest layers near the surface in order to accurately resolve rainfall-runoff-infiltration partitioning.

The water table position was set to 1.5 m below the surface based on available piezometric field data. Given the importance of soil moisture, some preliminary tests were conducted by simulating the artificial event with three different water table depths as initial condition and considering evapotranspiration (ET) or not. The average ET flux for April for the years 1996 to 2007 is $2.98e^{-8} \text{ m.s}^{-1}$ (Météo-France). Figures 6A and 6B show that evapotranspiration has no effect on surface water volume evolution through time but its influences on the average moisture in the first 50 cm of soil is apparent as early as the first simulation hours. Concerning the various water table depths, there is a clear difference in average moisture between the 0.5 m, 1 m, 1.5 m water table depth simulations, however all dynamics are similar. This parameter does not have a big impact

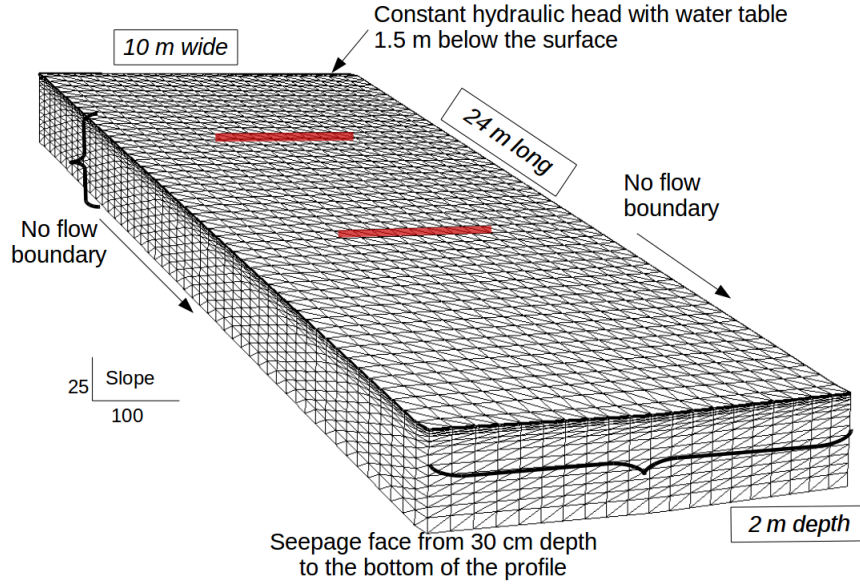


Figure 5: 3D mesh of the simulated area with applied boundary conditions for the CATHY model (mesh: 50 cm * 50 cm and 15 soil layers). Gutters 1 and 2 are represented in red.

187 on surface water volume (Figure 6B) and will be kept fixed for the rest of the study.

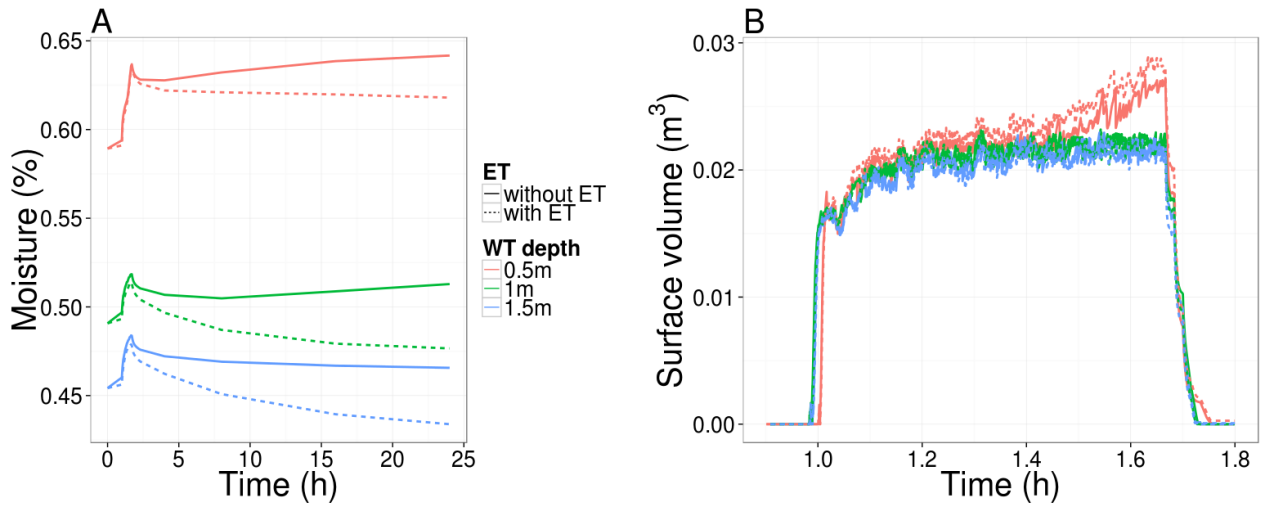


Figure 6: Model setup preliminary tests with various water table depth (WT depth) and evapotranspiration (ET) during the artificial event of 2006/04/13. (A) : average moisture evolution in the first 50 cm of soil through time. (B) : surface water volume evolution through time.

3. Results and discussion

3.1. Effect of subsurface heterogeneity

The first step of our analysis focuses on subsurface heterogeneity and is performed on the monitored artificial event (Figure 2 A) for the seven subsurface K_s scenarios (Table 2) and the smooth hillslope (no land surface microtopography) configuration.

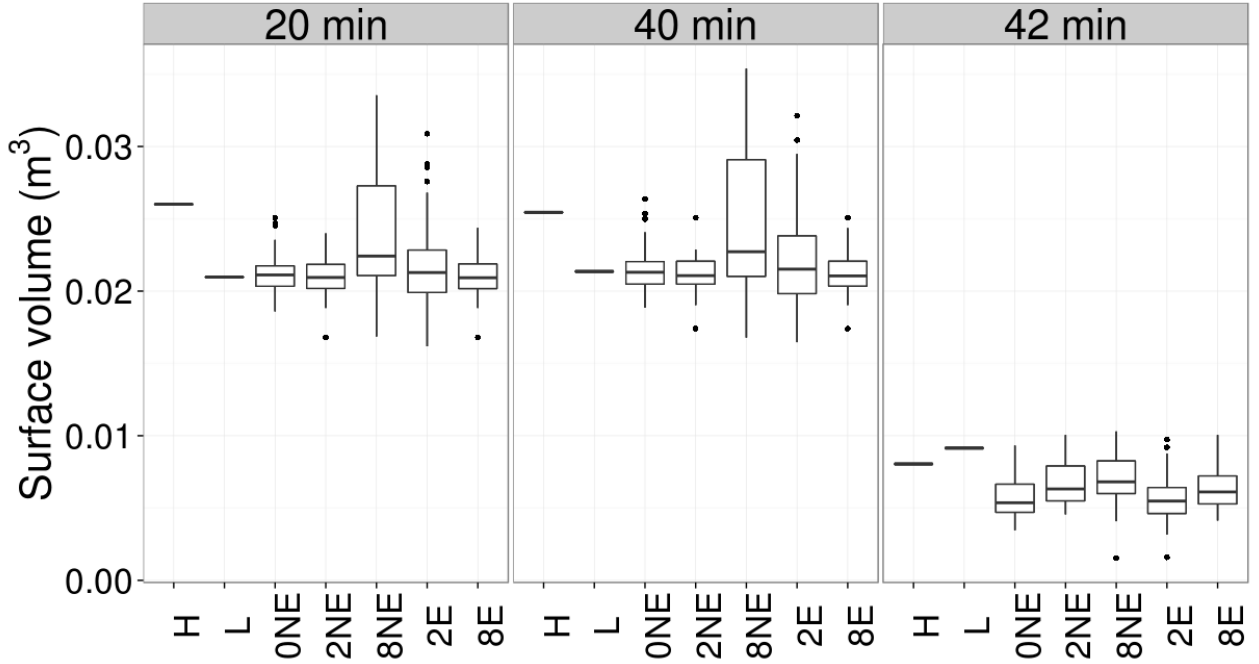


Figure 7: Boxplot of surface water volume at time 20 min, 40 min (end of water input, see Figure 2 A) and 42 min for the seven K_s scenarios during the artificial event of 2006/04/13. The boxplot results for the 5 statistically heterogeneous scenarios are derived from the 60 realizations that were run for each of these cases.

Figure 7 reports the boxplots of volume of water on the surface, defined as the integral of positive pressure head in regards to the surface, at three times: 20 min (middle of the runoff event), 40 min (end of the runoff event) and 42 min (after the end of the event and before all surface water has infiltrated). Globally, the timing trend is quite homogeneous: the volume of surface water is constant on average during the runoff event and decreases rapidly by the end of the runoff injection at gutter 1. Comparing the homogeneous (H) and layered heterogeneity (L) scenarios, the surface water volume seems to directly depend on the conductivity of the first soil horizon: during the runoff event there is 0.005 m^3 more water on the surface for the homogeneous scenario (with $K_s = 4.64\text{e-}5 \text{ m.s}^{-1}$) than for the layered scenario that has a higher K_s ($1.88\text{e-}4 \text{ m.s}^{-1}$) in the first horizon. After the injection period this difference decreases and the surface volumes for the H and L simulations are almost equal. For the statistically heterogeneous scenarios, the global mean of the surface water volume follows the L scenario, which indicates again a strong link with average K_s value of the first soil

horizon. However, the average of surface water volume stays stable for all heterogeneous scenarios : K_s spatial variability has little influence on this variable. Scenario 8NE (8 m correlation length, no enforcement) stands out as the configuration that produced the most variable and high response in terms of surface water volume over its 60 realizations.

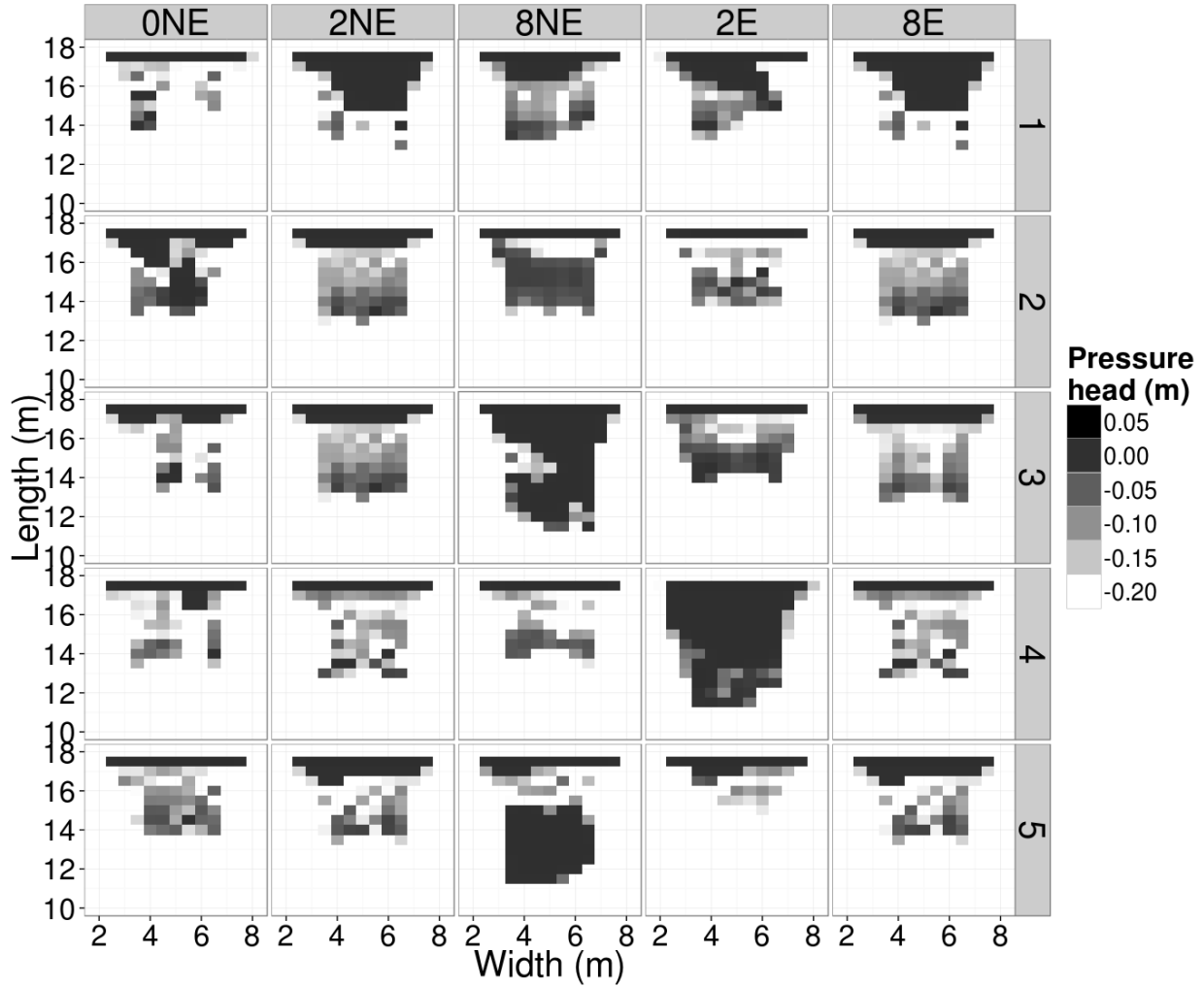


Figure 8: Surface pressure head at $t = 40$ min for five randomly chosen conductivity realizations from each heterogeneous K_s scenario during the artificial event of 2006/04/13. Only the experimental plot is represented (see Figure 1), and the axes are given with respect to the model domain.

In addition to its volume, the spatial repartitioning of surface water can also be qualitatively analysed via information obtained from the granular matrix sensors. The GMS data (not shown) indicate a spatial heterogeneity of the surface runoff and a relatively low temporal variability. The simulated spatial surface water repartitioning is shown in Figure 8 in terms of surface pressure head for five realizations of each of the statistically heterogeneous scenarios at $t = 40$ min. Because the hillslope is smooth, the H and L scenarios, with horizontally homogeneous soils, produced, as expected, a uniform ponding and therefore are not shown. The

resulting nonuniform pressure head distributions for all heterogeneous scenarios correspond to the evidence from the GMS observations. As with the surface water volume, the most highly variable ponding patterns (surface pressure heads greater than zero) occur for scenario 8NE. Because the subsurface heterogeneity is randomly generated, none of the simulated ponding patterns show clear runoff pathways. K_s variability, whether between scenarios or realizations, exerts a major influence on surface pressure, and thus on runoff. For some simulations (e.g., scenario 2NE realizations 1 and 5 and scenario 2E realizations 3 and 5, Figure 8) the surface water does not flow more than 3 or 4 m downslope from the injection point at gutter 1. This has consequences on the infiltration process, discussed next.

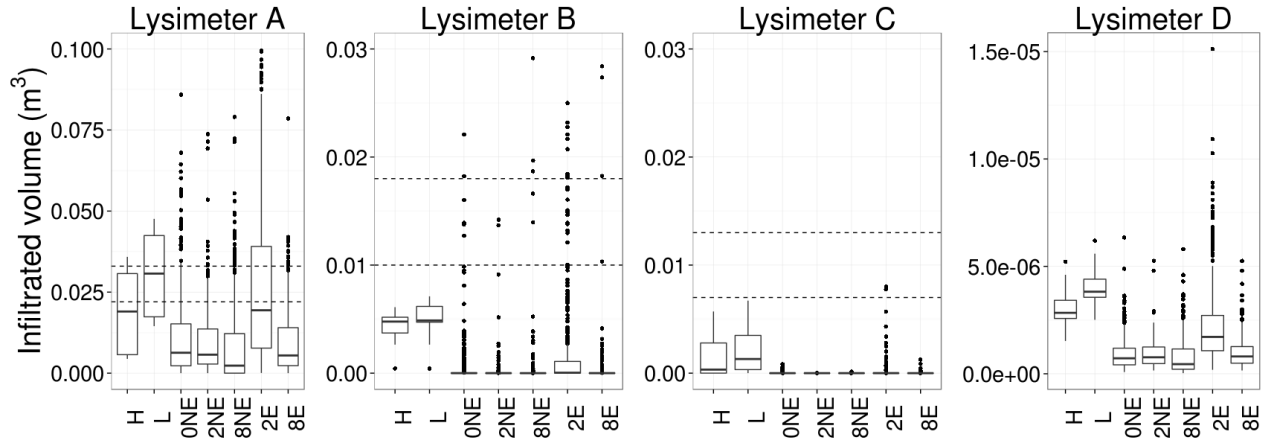


Figure 9: Boxplot of infiltrated volume at the four lysimeter positions and $t = 60$ min for the seven scenarios of K_s distribution during the artificial event of 2006/04/13. The simulated values are calculated at 50 cm depth along each of the 9-node transects that align with the lysimeter positions (see Figure 1). The dotted horizontal lines show the range of the measured data.

Figure 9 shows the volume infiltrated in the four lysimeters (see Figure 1) 60 min after the end of the simulation. On the field, each lysimeter is composed of two compartments, which provide two volume values, represented of Figure 9 by the two dotted lines. Note that the volumes measured and simulated at lysimeter D are quite negligible compared to the volumes at lysimeters A, B and C, and that more generally the average infiltrated volume decreases greatly in progressing downslope from lysimeter position A to D. For each lysimeter, the range of infiltrated volumes across the 7 scenarios varies over a much narrower range than from one lysimeter to the next. In contrast to the results for surface water volume, the most variable scenario here is not 8NE but 2E. This implies that the first 50 cm of soil can drastically alter trends observed at the surface. The simulation generally conforms to the field data in lysimeter A and underestimates infiltration in lysimeters B, C and D.

In order to examine the interactions between subsurface and surface heterogeneity in the second part of this study, we will focus on a heterogeneous scenario. On the basis of the lysimeter results, scenario 2E was selected among all heterogeneous scenarios and was applied for the natural rain event of 2004/09/12.

3.2. Effect of surface and subsurface heterogeneity

Similarly to the first step of the study, we first compare simulated surface water volume at various times (Figure 10): 15 min (first quarter of the natural event), 31 min (during the hydrograph peak) and 60 min (at the end of the event). The global trend follows a logical sequence for all three microtopography scenarios. At $t = 15$ min, the surface water volume is less than 0.01 m^3 , a relatively insignificant amount corresponding to less than 0.05 mm over the entire domain. At $t = 31$ min, during runoff generation, the surface water volume reaches a maximum of 0.6 m^3 (average of 2.5 mm of water over the entire simulated surface). By the end of the event, the surface water volume decreases rapidly, which was already observed in the first step. Besides this general trend, it can be seen that the level of ponding increases as the degree of elevation fluctuations increases.

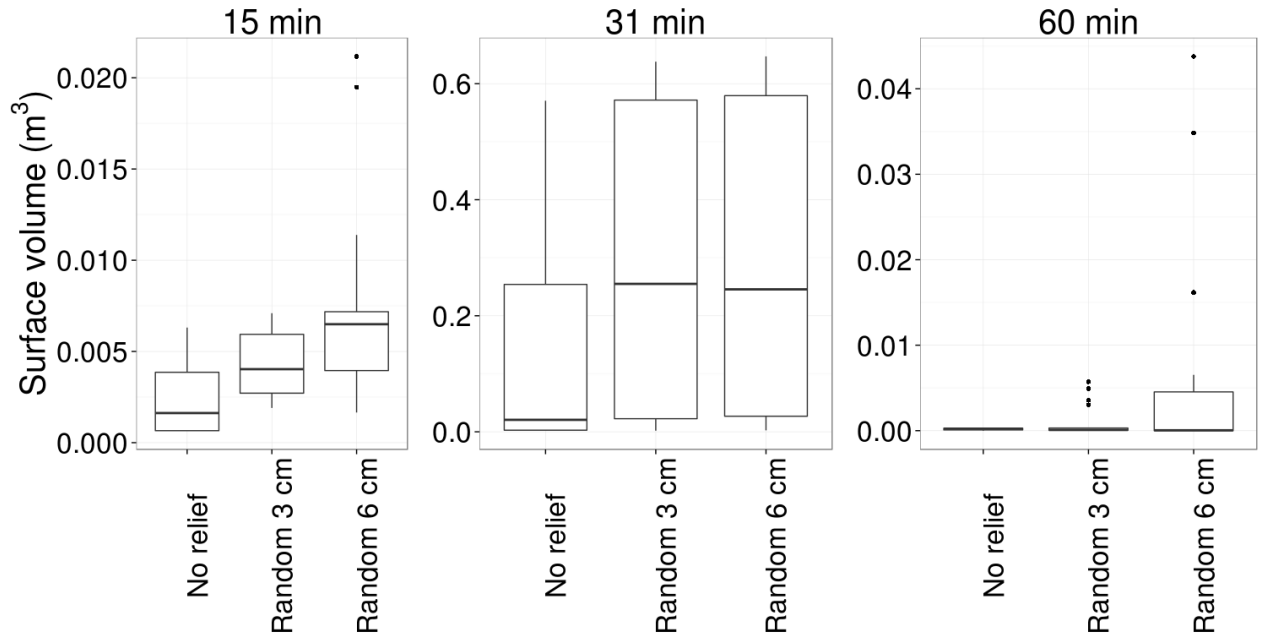


Figure 10: Boxplot of surface water volume at three times: 15 min, 31 min (output hydrograph peak) and 60 min for the three scenarios of microtopography heterogeneity during the natural event of 2004/09/12.

In Figure 11 A, runoff pathways are represented at $t = 31$ min, the peak of the output hydrograph at gutter 2. In contrast to the first part of the study with a smooth hillslope (Figure 8), preferential runoff pathways are observable when there is microtopographic relief (MT1 to MT5). There is a higher sensitivity to subsurface heterogeneity than to surface heterogeneity, as the variability is greater column-wise (different K_s realizations) than row-wise (MT scenarios). Indeed, the pressure head standard deviation for each node column-wise is three times higher (around 0.01 m) than row-wise (around 0.003 m). The same is also true for the hydrograph response in Figure 11B, and indeed in this case there is also not a great difference between the smooth hillslope, 3 cm microtopography, and 6 cm microtopography cases. This may be due to runoff

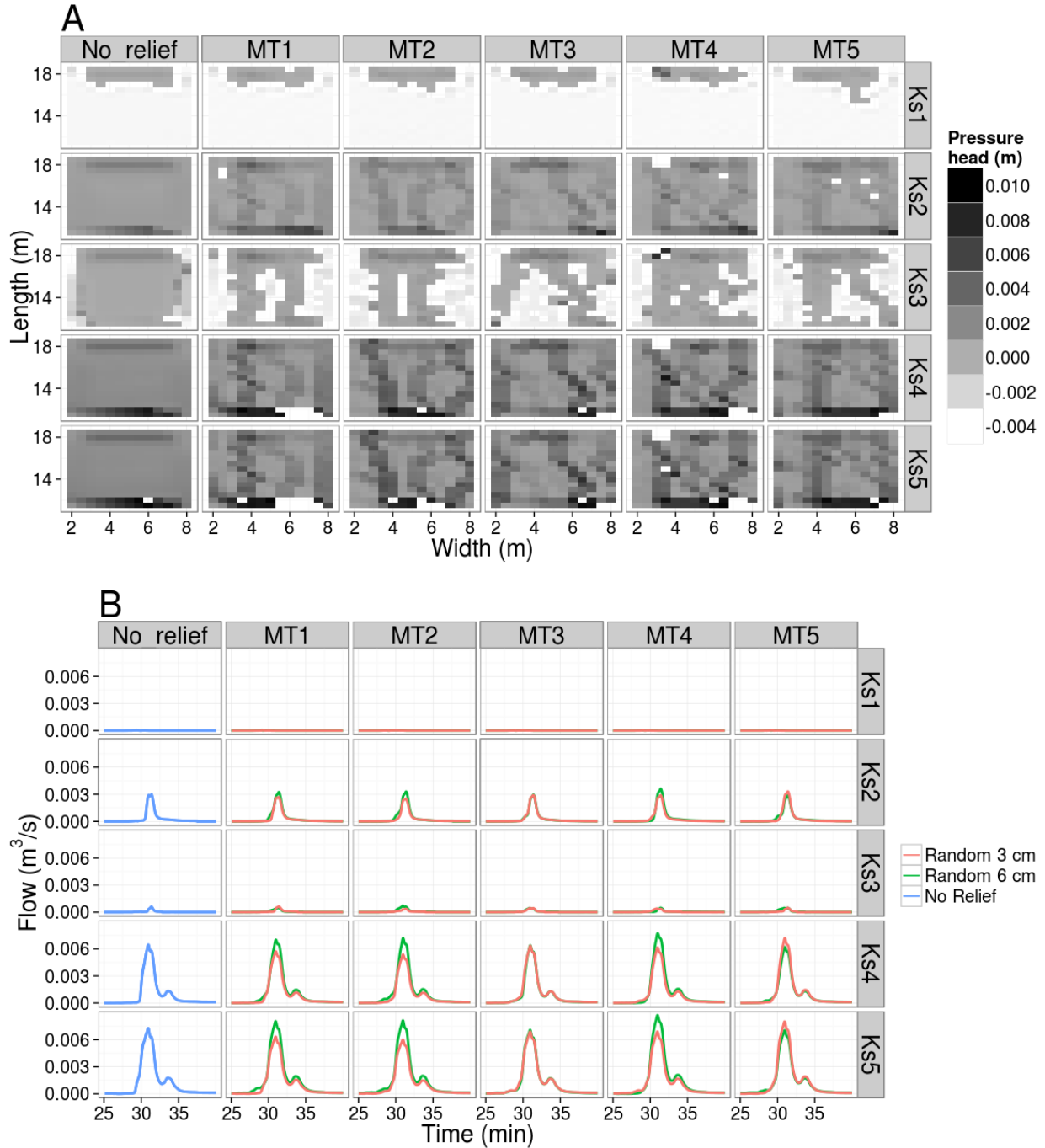


Figure 11: (A): Surface pressure head (m) at $t=31$ min for the smooth hillslope and for five realizations of the 6 cm microtopography average elevation scenario during the natural event of 2004/09/12. (B): hydrograph output at gutter 2 for all microtopography scenarios during the same event.

response in the surface model being more sensitive to the routing (hydraulic geometry) parameters than to the microtopography characteristics. Surface runoff pathways present different shapes depending on whether the area is flat or not (see figure 11A). Areas with microtopography (as opposed to flat areas) influence the runoff

pathway shape by concentrating flows, whereas the surface output hydrograph stays the same (see figure 11A, first column versus all others) : on non-flat areas, a same volume of water infiltrates on a smaller area.

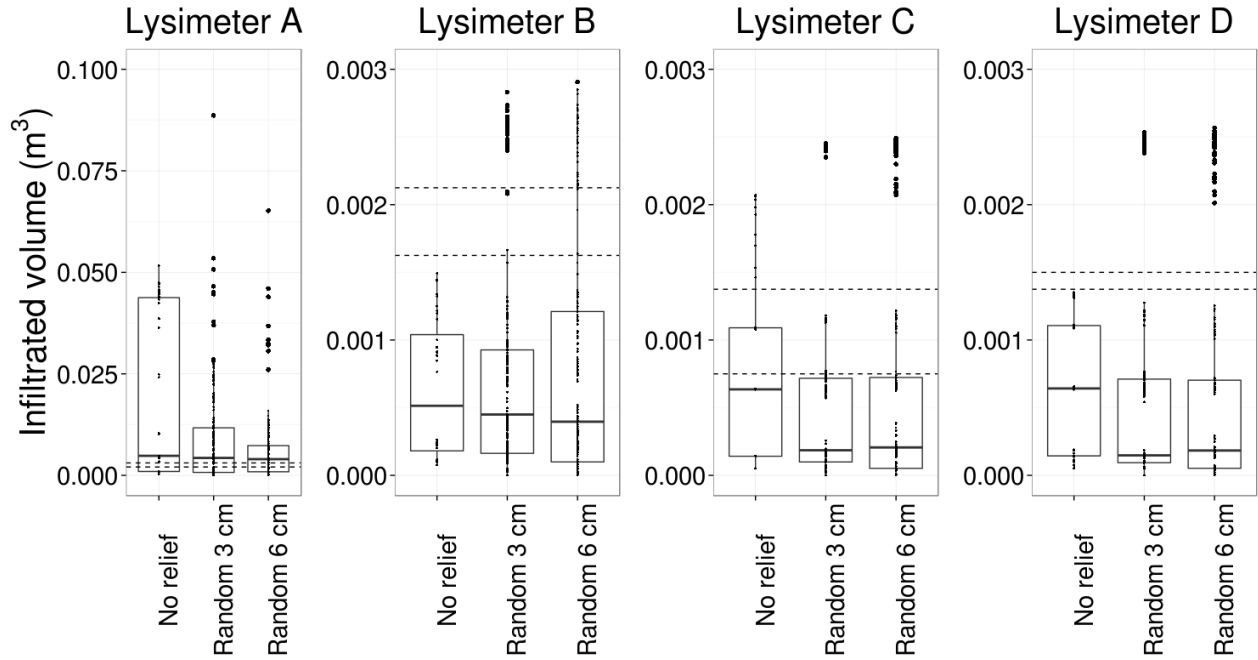


Figure 12: Boxplot of infiltrated volume at the four lysimeter positions and $t = 90$ min for the three microtopography scenarios during the artificial event of 2004/08/12. The simulated values are calculated at 50 cm depth along each of the 9-node transects that align with the lysimeter positions (see Figure 1). The dotted horizontal lines show the range of the measured data.

Figure 12 shows the infiltration volumes in lysimeters A, B, C and D after 90 min (30 min after the end of the event). As with the runoff hydrograph response in Figure 11B, the lysimeter results for the 3 cm and 6 cm microtopography scenarios are comparable in volume and degree of variability. The infiltrated volume for the simulation with a smooth soil surface is higher than with the rough surfaces for all 4 lysimeters, consistent with the lower surface volumes reported in Figure 10 for the smooth hillslope case. Finally, as with the analysis of subsurface heterogeneity in the previous step reported in Figure 9, we again see a general overestimation of the simulated infiltrated volume for lysimeter A compared to the measured data and an underestimation for lysimeters B, C and D.

4. Conclusions

In this paper, the effect of surface and subsurface heterogeneity representation on water flow in a vegetative buffer strip was assessed. The seven scenarios of saturated hydraulic conductivity simulated with the CATHY model confirmed that conductivity heterogeneity has a significant impact on the buffer strip's capacity to infiltrate incoming surface runoff. Moreover, enforced scenarios were more consistent with the observations of surface and subsurface responses than the non enforced ones. This result strongly supports the necessity to

carefully parameterize hydraulic conductivity by adding information from measurements. In a second step, we examined both surface and subsurface heterogeneity via scenarios combining topographic relief and K_s distributions. The results indicate that the hydrological responses of the buffer strip are much less sensitive to microtopography variability than to K_s variability. This conclusion was observed for variations in both elevation mean and spatial distribution. Microtopography can thus be represented by synthetic distributions, so long as it is not entirely neglected, as is often done due to lack of data.

This study focused on K_s and microtopography in representing subsurface and surface heterogeneity, given their importance as suggested by the literature. Other soil characteristics may also be influential, such as initial soil moisture, porosity, roughness, and retention curve parameters. This study approaches the sensitivity analysis idea with few parameters. A rigorous sensitivity analysis of surface runoff and infiltration responses to a wider set of parameters will be conducted in a subsequent study, and will include also an investigation of potential correlations between surface and subsurface heterogeneity. Preferential transfer often accelerates pesticide transfer, depending on the soil structure. Moreover, solute and sediment transfers are in strong interaction with water fluxes on buffer strips. By deliberately focusing on hydrological processes alone in this present study, we have been able to elucidate the combined effects of soil surface and subsurface heterogeneity, at the scale and in the context of a buffer strip. This first study using a physically-based coupled model to examine both surface and subsurface heterogeneity factors has provided some key insights into what variables should be taken into account or neglected in order to properly represent integrated hydrologic fluxes in a vegetative filter.

Acknowledgment

The authors acknowledge the geostatistical help and advices of E. Leblois. The research for this paper was in part supported by the CMIRA Explora'Doc grant from the Region Auvergne-Rhône-Alpes and the LEFE/MANU project ADIMAP.

References

- [1] N. Poletika, P. Coody, G. Fox, G. Sabbagh, S. Dolder, J. White, Chlorpyrifos and atrazine removal from runoff by vegetated filter strips: Experiments and predictive modeling, *Journal of Environmental Quality* 38 (3) (2009) 1042–1052. doi:10.2134/jeq2008.0404.
- [2] B. Real, J. Mezeray, G. l. Henaaff, M. Roettele, et al., Topps-prowadis project: development of diagnosis methods and proposal of practical solutions in order to reduce transfers of plant protection product from run-off and erosion., in: 22e Conférence du COLUMA. Journées Internationales sur la Lutte contre les

- Mauvaises Herbes, Dijon, France, 10-12 décembre 2013., Association Française de Protection des Plantes (AFPP), 2013, pp. 672–681.
- [3] M. G. Dosskey, Toward quantifying water pollution abatement in response to installing buffers on crop land, *Environmental Management* 28 (5) (2001) 577–598. doi:10.1007/s002670010245.
- [4] A. L. Fox, D. E. Eisenhauer, M. Dosskey, Modeling water and sediment trapping by vegetated filters using VFSMOD: Comparing methods for estimating infiltration parameters, USDA Forest Service/UNL Faculty Publications. (2005) nadoi:10.13031/2013.18934.
- [5] A. Carter, Herbicide movement in soils: principles, pathways and processes, *Weed Research* 40 (1) (2000) 113–122. doi:10.1046/j.1365-3180.2000.00157.x.
- [6] J.-G. Lacas, Processus de dissipation des produits phytosanitaires dans les zones tampons enherbées: étude expérimentale et modélisation en vue de limiter la contamination des eaux de surface, Ph.D. thesis, Montpellier 2 (2005).
- [7] J.-G. Lacas, N. Carluer, M. Voltz, Efficiency of a grass buffer strip for limiting diuron losses from an uphill vineyard towards surface and subsurface waters, *Pedosphere* 22 (4) (2012) 580–592. doi:10.1016/S1002-0160(12)60043-5.
- [8] J.-G. Lacas, M. Voltz, V. Gouy, N. Carluer, J.-J. Gril, Using grassed strips to limit pesticide transfer to surface water: a review, *Agronomy for Sustainable Development* 25 (2) (2005) 253–266.
- [9] D. Lee, T. D. Dillaha, J. H. Sherrard, Modeling phosphorus transport in grass buffer strips, *Journal of Environmental Engineering* 115 (2) (1989) 409–427. doi:10.1061/(ASCE)0733-9372(1989)115:2(409).
- [10] R. Munoz-Carpena, J. E. Parsons, J. Gilliam, Modeling hydrology and sediment transport in vegetative filter strips, *Journal of Hydrology* 214 (14) (1999) 111–129. doi:10.1016/S0022-1694(98)00272-8.
- [11] J. Simunek, M. Sejna, M. van Genuchten, The HYDRUS-2D software package for simulating two-dimensional movement of water, heat, and multiple solutes in variably-saturated media, Version 2.0, US Salinity Laboratory, USDA, ARS, Riverside.
- [12] C. Yu, C. Zheng, Hydrus: Software for flow and transport modeling in variably saturated media, *Ground Water* 48 (6) (2010) 787–791. doi:10.1111/j.1745-6584.2010.00751.x.
- [13] J. M. Koehne, T. Woehling, V. Pot, P. Benoit, S. Leguedois, Y. L. Bissonnais, J. Simunek, Coupled simulation of surface runoff and soil water flow using multi-objective parameter estimation, *Journal of Hydrology* 403 (12) (2011) 141–156. doi:10.1016/j.jhydro1.2011.04.001.

- [14] M. Abu-Zreig, Factors affecting sediment trapping in vegetated filter strips: simulation study using VFS-MOD, *Hydrological Processes* 15 (8) (2001) 1477–1488. doi:10.1002/hyp.220.
- [15] A. Sovik, P. Aagaard, Spatial variability of a solid porous framework with regard to chemical and physical properties, *Geoderma* 113 (1) (2003) 47–76. doi:10.1016/S0016-7061(02)00315-4.
- [16] M. Herbst, B. Diekkrueger, J. Vanderborght, Numerical experiments on the sensitivity of runoff generation to the spatial variation of soil hydraulic properties, *Journal of Hydrology* 326 (1) (2006) 43–58. doi:10.1016/j.jhydrol.2005.10.036.
- [17] M. M. Gribb, Parameter estimation for determining hydraulic properties of a fine sand from transient flow measurements, *Water Resources Research* 32 (7) (1996) 1965–1974. doi:10.1029/96WR00894.
- [18] T.-C. J. Yeh, J. Zhang, A geostatistical inverse method for variably saturated flow in the vadose zone, *Water Resources Research* 32 (9) (1996) 2757–2766. doi:10.1029/96WR01497.
- [19] S. Boateng, Evaluation of probabilistic flow in two unsaturated soils, *Hydrogeology Journal* 9 (6) (2001) 543–554. doi:10.1007/s10040-001-0164-6.
- [20] J. Mertens, H. Madsen, M. Kristensen, D. Jacques, J. Feyen, Sensitivity of soil parameters in unsaturated zone modelling and the relation between effective, laboratory and in situ estimates, *Hydrological Processes* 19 (8) (2005) 1611–1633. doi:10.1002/hyp.5591.
- [21] J. Simunek, M. van Genuchten, M. M. Gribb, J. W. Hopmans, Parameter estimation of unsaturated soil hydraulic properties from transient flow processes, *Soil and Tillage Research* 47 (1) (1998) 27–36. doi:10.1016/S0167-1987(98)00069-5.
- [22] F. Abbasi, J. Feyen, M. T. van Genuchten, Two-dimensional simulation of water flow and solute transport below furrows: model calibration and validation, *Journal of Hydrology* 290 (1) (2004) 63–79. doi:10.1016/j.jhydrol.2003.11.028.
- [23] C. Dages, M. Voltz, P. Ackerer, Parameterization and evaluation of a three-dimensional modelling approach to water table recharge from seepage losses in a ditch, *Journal of Hydrology* 348 (3) (2008) 350–362. doi:10.1016/j.jhydrol.2007.10.004.
- [24] X. Liang, Z. Xie, A new surface runoff parameterization with subgrid-scale soil heterogeneity for land surface models, *Advances in Water Resources* 24 (9–10) (2001) 1173–1193. doi:10.1016/S0309-1708(01)00032-X.
- [25] V. Polyakov, A. Fares, M. H. Ryder, Precision riparian buffers for the control of nonpoint source pollutant loading into surface water: A review, *Environmental Reviews* 13 (3) (2005) 129–144. doi:10.1139/a05-010.

- [26] K. Moser, C. Ahn, G. Noe, Characterization of microtopography and its influence on vegetation patterns in created wetlands, *Wetlands* 27 (4) (2007) 1081–1097. doi:10.1672/0277-5212(2007)27[1081:COMAII]2.0.CO;2.
- [27] B. P. Mohanty, M. D. Ankeny, R. Horton, R. S. Kanwar, Spatial analysis of hydraulic conductivity measured using disc infiltrometers, *Water Resources Research* 30 (9) (1994) 2489–2498. doi:10.1029/94WR01052.
- [28] K. J. Beven, E. F. Wood, M. Sivapalan, On hydrological heterogeneity : Catchment morphology and catchment response, *Journal of Hydrology* 100 (13) (1988) 353–375. doi:10.1016/0022-1694(88)90192-8.
- [29] M. B. Ceddia, S. R. Vieira, A. L. O. Villela, L. d. S. Mota, L. H. C. Anjos, D. F. Carvalho, Topography and spatial variability of soil physical properties, *Scientia Agricola* 66 (2009) 338–352. doi:10.1590/S0103-90162009000300009.
- [30] D. Mulla, Variability in soil properties from soil classification, in: A. W. Warrick (Ed.), *Soil Physics Companion*, Taylor & Francis Group, Boca Raton, 2010, Ch. 9, pp. 343–344.
- [31] D. A. Woolhiser, R. E. Smith, J.-V. Giraldez, Effects of spatial variability of saturated hydraulic conductivity on Hortonian overland flow, *Water Resources Research* 32 (3) (1996) 671–678. doi:10.1029/95WR03108.
- [32] A. Sole-Benet, A. Calvo, A. Cerda, R. Lazaro, R. Pini, J. Barbero, Influences of micro-relief patterns and plant cover on runoff related processes in badlands from Tabernas (SE Spain), *Catena* 31 (1-2) (1997) 23–38. doi:10.1016/S0341-8162(97)00032-5.
- [33] P. Van Der Keur, B. V. Iversen, Uncertainty in soil physical data at river basin scale ? a review, *Hydrology and Earth System Sciences Discussions* 10 (6) (2006) 889–902.
URL <https://hal.archives-ouvertes.fr/hal-00305034>
- [34] J. Sobieraj, H. Elsenbeer, G. Cameron, Scale dependency in spatial patterns of saturated hydraulic conductivity, *Catena* 55 (1) (2004) 49–77. doi:10.1016/S0341-8162(03)00090-0.
- [35] P. Cook, G. Walker, I. Jolly, Spatial variability of groundwater recharge in a semiarid region, *Journal of Hydrology* 111 (1) (1989) 195–212. doi:10.1016/0022-1694(89)90260-6.
- [36] D. Russo, E. Bresler, Soil hydraulic properties as stochastic processes: I. an analysis of field spatial variability, *Soil Science Society of America Journal* 45 (4) (1981) 682–687. doi:10.2136/sssaj1981.03615995004500040002x.

- [37] L. Chen, S. Sela, T. Svoray, S. Assouline, The role of soil-surface sealing, microtopography, and vegetation patches in rainfall-runoff processes in semiarid areas, *Water Resources Research* 49 (9) (2013) 5585–5599. doi:10.1002/wrcr.20360.
- [38] S. Frei, G. Lischied, J. Fleckenstein, Effects of microtopography on surface subsurface exchange and runoff generation in a virtual riparian wetland. a modeling study, *Advances in Water Resources* 33 (11) (2010) 1388–1401. doi:10.1016/j.advwatres.2010.07.006.
- [39] M. Seyfried, Spatial variability constraints to modeling soil water at different scales, *Geoderma* 85 (2–3) (1998) 231–254. doi:10.1016/S0016-7061(98)00022-6.
- [40] A. Samouelian, I. Cousin, C. Dages, A. Frison, G. Richard, Determining the effective hydraulic properties of a highly heterogeneous soil horizon, *Vadose Zone Journal* 10 (1) (2011) 450–458. doi:doi:10.2136/vzj2010.0008.
- [41] G. Dagan, E. Bresler, Unsaturated flow in spatially variable fields: 1. derivation of models of infiltration and redistribution, *Water Resources Research* 19 (2) (1983) 413–420. doi:10.1029/WR019i002p00413.
- [42] H. M. Abdou, M. Flury, Simulation of water flow and solute transport in free-drainage lysimeters and field soils with heterogeneous structures, *European Journal of Soil Science* 55 (2) (2004) 229–241. doi:10.1046/j.1365-2389.2004.00592.x.
- [43] J. R. Craig, G. Liu, E. D. Soulis, Runoff infiltration partitioning using an upscaled Green-Ampt solution, *Hydrological Processes* 24 (16) (2010) 2328–2334. doi:10.1002/hyp.7601.
- [44] R. S. Govindaraju, C. Corradini, R. Morbidelli, Local- and field-scale infiltration into vertically non-uniform soils with spatially-variable surface hydraulic conductivities, *Hydrological Processes* 26 (21) (2012) 3293–3301. doi:10.1002/hyp.8454.
- [45] D. Pasetto, G.-Y. Niu, L. Pangle, C. Paniconi, M. Putti, P. A. Troch, Impact of sensor failure on the observability of flow dynamics at the Biosphere 2 LEO hillslopes, *Advances in Water Resources* 86 (2015) 327–339. doi:10.1016/j.advwatres.2015.04.014.
- [46] B. Zinn, C. F. Harvey, When good statistical models of aquifer heterogeneity go bad: A comparison of flow, dispersion, and mass transfer in connected and multivariate Gaussian hydraulic conductivity fields, *Water Resources Research* 39 (3) (2003) na. doi:10.1029/2001WR001146.
- [47] M. Antoine, M. Javaux, C. L. Bielders, Integrating subgrid connectivity properties of the microtopography in distributed runoff models, at the interrill scale, *Journal of Hydrology* 403 (2011) 213–223. doi:10.1016/j.jhydrol.2011.03.027.

- [48] W. M. Appels, P. W. Bogaart, S. E. van der Zee, Influence of spatial variations of microtopography and infiltration on surface runoff and field scale hydrological connectivity, *Advances in Water Resources* 34 (2) (2011) 303–313. doi:10.1016/j.advwatres.2010.12.003.
- [49] J. Yang, X. Chu, A new modeling approach for simulating microtopography-dominated, discontinuous overland flow on infiltrating surfaces, *Advances in Water Resources* 78 (2015) 80–93. doi:10.1016/j.advwatres.2015.02.004.
- [50] P. M. Atkinson, N. J. Tate, Spatial scale problems and geostatistical solutions: A review, *The Professional Geographer* 52 (4) (2000) 607–623. doi:10.1111/0033-0124.00250.
- [51] S. E. Thompson, G. G. Katul, A. Porporato, Role of microtopography in rainfall-runoff partitioning: An analysis using idealized geometry, *Water Resources Research* 46 (7) (2010) na. doi:10.1029/2009WR008835.
- [52] S. Anderton, J. Latron, F. Gallart, Sensitivity analysis and multi-response, multi-criteria evaluation of a physically based distributed model, *Hydrological Processes* 16 (2) (2002) 333–353. doi:10.1002/hyp.336.
- [53] C. Paniconi, M. Putti, Physically based modeling in catchment hydrology at 50: Survey and outlook, *Water Resources Research* 51 (9) (2015) 7090–7129. doi:10.1002/2015WR017780.
- [54] M. Camporese, C. Paniconi, M. Putti, S. Orlandini, Surface-subsurface flow modeling with path-based runoff routing, boundary condition-based coupling, and assimilation of multisource observation data, *Water Resources Research* 46 (2) (2010) W02512. doi:10.1029/2008WR007536.
- [55] C. Paniconi, M. Putti, A comparison of Picard and Newton iteration in the numerical solution of multidimensional variably saturated flow problems, *Water Resources Research* 30 (12) (1994) 3357–3374. doi:10.1029/94WR02046.
- [56] S. Orlandini, G. Moretti, M. Franchini, B. Aldighieri, B. Testa, Path-based methods for the determination of nondispersive drainage directions in grid-based digital elevation models, *Water Resources Research* 39 (6) (2003) na.
- [57] M. C. Peel, B. L. Finlayson, T. A. McMahon, Updated world map of the Köppen-Geiger climate classification, *Hydrol. Earth Syst. Sci.* 11 (5) (2007) 1633–1644. doi:10.5194/hess-11-1633-2007.
- [58] R. VandenBogaert, Typologie des sols du bassin versant de la Morcille, caractérisation de leurs propriétés hydrauliques et test de fonctions de pedotransfert., Master's thesis, Université Pierre et Marie Curie & AgroParisTech (2011).

- [59] E. P. Eldredge, C. C. Shock, T. D. Stieber, Calibration of granular matrix sensors for irrigation management, *Agronomy Journal* 85 (6) (1993) 1228–1232. doi:10.2134/agronj1993.00021962008500060025x.
- [60] M. T. van Genuchten, A closed-form equation for predicting the hydraulic conductivity of unsaturated soils, *Soil Science Society of America Journal* 44 (5) (1980) 892–898.
- [61] E. Leblois, J.-D. Creutin, Space-time simulation of intermittent rainfall with prescribed advection field: Adaptation of the turning band method, *Water Resources Research* 49 (6) (2013) 3375–3387. doi:10.1002/wrcr.20190.
- [62] G. Pardini, F. Gallart, A combination of laser technology and fractals to analyse soil surface roughness, *European Journal of Soil Science* 49 (2) (1998) 197–202. doi:10.1046/j.1365-2389.1998.00149.x.
- [63] F. Darboux, C. Gascuel-Oudou, P. Davy, Effects of surface water storage by soil roughness on overland-flow generation, *Earth Surface Processes and Landforms* 27 (3) (2002) 223–233. doi:10.1002/esp.313.
- [64] F. S. J. Martinez, J. Caniego, A. Guber, Y. Pachepsky, M. Reyes, Multifractal modeling of soil micro-topography with multiple transects data, *Ecological Complexity* 6 (3) (2009) 240–245. doi:10.1016/j.ecocom.2009.05.002.
- [65] J. K. Mitchell, B. A. Jones, Microrelief surface depression storage: Analysis of models to describe the depth-storage function1, *Journal of the American Water Resources Association* 12 (6) (1976) 1205–1222. doi:10.1111/j.1752-1688.1976.tb00256.x.
- [66] G. Govers, I. Takken, K. Helming, Soil roughness and overland flow, *Agronomie* 20 (2) (2000) 131–146. doi:10.1051/agro:2000114.
- [67] R. Munoz-Carpena, G. A. Fox, G. J. Sabbagh, Parameter importance and uncertainty in predicting runoff pesticide reduction with filter strips, *Journal of environmental quality* 39 (2) (2010) 630–641.

Effect of surface and subsurface heterogeneity on the hydrological response of a grassed buffer zone

Highlights :

- Heterogeneous saturated conductivity (Ks) reflects the complexity of buffer strips.
- Field data-enforced model parameterization improves consistency with observations.
- Hydrological responses are more sensitive to Ks than to microtopography variability.

Email address: laura.gatel@irstea.fr (Laura Gatel)